Exploration of BioMat-X

Open Exploration

Open Access Original Article

Gum Arabic-assisted green synthesis of gold nanoparticles as fluorescence modulator for potential analytical applications

Ahmed T. Algahiny[1†], Omar S. Elmitwalli[1†], Deyari A. Kassim[1], G. Roshan Deen[1], Sultan Akhtar[2], Fryad Z. Henari[1*]

[1]Department Medical Sciences, Royal College of Surgeons in Ireland, Medical University of Bahrain, P.O. Box 15503, Busaiteen 228, Kingdom of Bahrain

[2]Department of Biophysics, Institute for Research and Medical Consultations (IRMC), Imam Abdulrahman Bin Faisal University, P.O. Box 1982, Dammam 31441, Saudi Arabia

[†]These authors contributed equally to this work.

***Correspondence:** Fryad Z. Henari, Department Medical Sciences, Royal College of Surgeons in Ireland, Medical University of Bahrain, P.O. Box 15503, Busaiteen 228, Kingdom of Bahrain. fzhenari@rcsi-mub.com

Academic Editor: Mohammad Tavakkoli Yaraki, Macquarie University, Australia

Received: February 8, 2024 **Accepted:** July 4, 2024 **Published:** July 28, 2024

Cite this article: Algahiny AT, Elmitwalli OS, Kassim DA, Deen GR, Akhtar S, Henari FZ. Gum Arabic-assisted green synthesis of gold nanoparticles as fluorescence modulator for potential analytical applications. Explor BioMat-X. 2024;1:190–201. https://doi.org/10.37349/ebmx.2024.00014

Abstract

Aim: To demonstrate a simple, eco-friendly, and cost-effective green method to synthesize gold nanoparticles (AuNPs) using the aqueous extract of gum Arabic (GA) as a reducing and stabilizing agent.

Methods: Green synthesis of nanoparticles, characterization by absorption, infra-red and fluorescence spectroscopy.

Results: The absorption spectrum (UV-Vis) showed an absorption peak ~522 nm corresponding to the surface plasmon resonance (SPR) absorption peak of AuNPs. Transmission electron microscopy (TEM) images revealed spherical-shaped nanoparticles with an average size of 15 nm. Fourier transform infrared (FTIR) analysis showed that the nanoparticles are coated with organic compounds that are present in GA. The fluorescence quenching properties of the AuNPs were assessed by monitoring their effects on fluorescence intensity of coumarin 153 (C153) dye. The fluorescence of the dye decreased with an increase in concentration of the nanoparticles. Upon addition of the protein bovine serum albumin (BSA) to the mixture the fluorescence increased (recovery) again.

Conclusions: The fluorescence quenching and recovery (turn-on/off system) is a valuable method for protein detection in solution. By observing the effect of BSA on the quenched fluorescence, this nanoparticle system shows promise in biomedicine, drug delivery and environmental monitoring.

Keywords

Green synthesis, gum Arabic, gold nanoparticles, fluorescence quenching, protein detection

Introduction

Many physical and chemical methods have been used to synthesize metallic nanoparticles (NPs). However, over the last decade, green synthesis of NPs has been favored over the traditional physical and chemical processes mainly due to the rising concern of using very expensive equipment and toxic chemical substances [1]. The green synthesis of metal NPs involves using different microorganisms such as bacteria, fungi, algae, and plants. The aqueous extracts of different parts of the plants such as leaves, flowers, roots, pods, and fruits have been widely explored [2, 3]. Extracts of a various range of plant species have been successfully employed in the synthesis of NPs and these include cinnamon [4], hibiscus [5], geranium [6], and gum Arabic (GA) [7, 8]. The phytochemicals present in the extracts act as reducing agents and stabilizers in the synthesis process of these metal NPs [3]. GA is the gum that is released from certain trees, such as the Acacia Senegal tree. GA is a polymeric material composed of glycoprotein and polysaccharide, consisting of amino acids and hydroxyl groups on the polymer chains that could reduce metal ions to metal NPs through oxidation reactions [7, 8].

Gold NPs (AuNPs) are among the many inorganic metal NPs that can be synthesized using various plant extracts. One distinctive feature of AuNPs is their unique surface plasmon resonance (SPR) peak absorption, which can vary when the size and shape of the NPs varies. The SPR arises when the incident light interacts with a free electron on the conduction band surface, causing the free electrons to oscillate in resonance with the frequency of the incident light. These optical properties can efficiently manipulate their applications in biological sciences, biomedicine, drug delivery, and environmental monitoring [9, 10]. The AuNPs have been widely used as fluorescence quenching agents due to their stability, sensitivity, and high absorption coefficient [9–11]. In addition, AuNPs have high quenching efficacy, giving them a distinct ability to bind dye molecules on to their surface, and developing an efficient, fluorescent-based assay based on AuNPs has been a particular area of interest [12]. AuNPs can quench the fluorescence emitted by fluorophores when they are in the vicinity of each other [10]. This phenomenon can be applied to investigate the binding of drugs to proteins and their transport, chemical and biological sensing, and to develop biosensors for monitoring of environmental pollutants [13, 14].

The fluorescence quenching by NPs is reportedly directed by various processes such as excited-state reactions, molecular rearrangements, energy transfer, ground-state complex formation, and collisional quenching [15]. The combination of AuNPs and fluorophore leads to a fluorescence activatable probe system, where the AuNP, or the quencher, acts as an acceptor, and the fluorophore acts as a donor [12]. These systems are particularly important in detecting the presence of proteins and oligonucleotides [12] in solution. The quenching effect of the AuNP on fluorophore molecules is distance-dependent, i.e., the quenching occurs if the distance between the two is small, and if the distance between the two is relatively large, mainly due to the presence of markers, then quenching decreases significantly with the recovery of fluorescence [12, 15].

In this study, AuNPs were synthesized using the aqueous extract of GA. The characteristics of the synthesized AuNPs were assessed using ultra-violet-visible (UV-Vis) spectroscopy, transmission electron microscopy (TEM) and Fourier transform infrared (FTIR). The AuNPs were used to explore the quenching of coumarin 153 (C153) dye. The Stern-Volmer equation was used to examine the quenching mechanism. The quenching process is discussed based on the excitation energy transfer between the dye and Au NPs. The recovery of the fluorescence quenching was investigated by adding bovine serum albumin (BSA) as a target marker to the AuNP-C153 dye mixture. The interaction between the AuNPs and BSA molecules allowed the dye molecules to desorb from the surface of AuNPs with recovery of fluorescence. To the best of our knowledge, AuNPs synthesized using GA has not been fully explored for fluorescence quenching and recovery using the protein, BSA.

Materials and methods

Materials

GA from the Acacia tree, gold (III) chloride trihydrate ($HAuCl_4$), sodium hydroxide, and BSA were purchased from Sigma-Aldrich and used as received. C153 dye (laser grade) was obtained from exciton. All aqueous samples were prepared using deionized water collected from a Millipore system.

Synthesis of AuNPs

The AuNPs was synthesized using a modified green method reported earlier [7]. Briefly, GA stock solution of 15 g/L was prepared by dissolving 0.375 g of the gum in 25 mL of water. Three samples were prepared by mixing various volumes of gold salt solution with a fixed volume of GA extract at 23°C. A 100 microliter of 0.5 M NaOH was added to each solution, followed by heating in a microwave oven (power 1,000 W) for 15 s. The change in color of the solution to deep purple after microwave irradiation confirmed the formation of AuNPs. The composition of the samples is presented in Table 1, and the synthesis methodology is illustrated in Figure 1.

Table 1. Composition of the mixture used in the synthesis of gold nanoparticles

Sample	GA extract (mL)	0.1 mM $HAuCl_4$ (mL)	0.5 M NaOH (L)	Final pH	Colour after heating
A	1	0.5	100	8.7	Purple
B	1	1.5	100	8.7	Purple
C	1	2.0	100	8.7	Purple

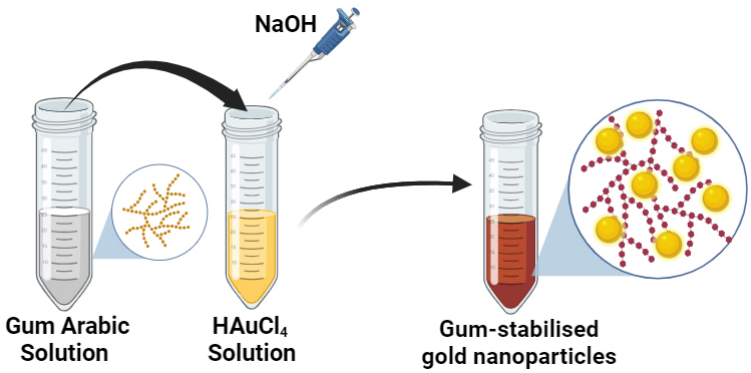

Figure 1. A schematic representation of gum-assisted synthesis of gold nanoparticles

Characterization

The formation of AuNPs was studied by measuring the absorbance of the samples using a double-beam Shimadzu UV-1800 spectrophotometer. The measurement was conducted after 30 min of preparation to allow sufficient time to complete the reaction. Sample B was chosen as a representative example to study the stability of the NPs in solution over time (4, 11, and 19 days). The size and morphology of the NPs were studied using TEM (FEI Morgagni 268, Czech Republic, operating voltage = 80 kV). The samples were prepared by placing a drop of the colloidal NPs on a carbon-support copper grid, followed by air drying. The electronic images of the AuNPs were obtained in the bright-field imaging mode. The FTIR spectra of GA and GA coated AuNPs were recorded using a Bruker Alpha spectrophotometer in the scanning range of 4,000–500 cm^{-1}. The samples were ground with dry potassium bromide (Spectroscopy grade, Sigma-Aldrich) and pressed to form a thin, transparent pellet.

Fluorescence quenching

The effect of GA-Au on the fluorescence of C153 dye was measured using a fluorometer (Shimadzu RF-1600). The fluorescence measurements were made by adding 2, 4, 6, 8, 10, 12, 14, and 16 µL of AuNPs from sample B to a fixed volume of the dye (2 mL). The fluorescence recovery of AuNPs-dye was investigated by

adding 0.5, 1.0 and 1.5 mL of 25 g/L of BSA solution to the sample containing 16 µL of AuNP + 1 mL dye. The volume of all mixtures was kept constant.

Results

The change in color of the sample solutions from light yellow to purple-red confirmed the formation of AuNPs (Figure 2a, inset). The color change is due to the excitation of surface plasmon electron oscillation at the conduction band of the NPs [8]. The characteristic SPR absorption peak is another indication of the formation of AuNPs. The colloidal solution remained clear with no precipitation. This indicated that the produced NPs were stable and uniformly dispersed [8].

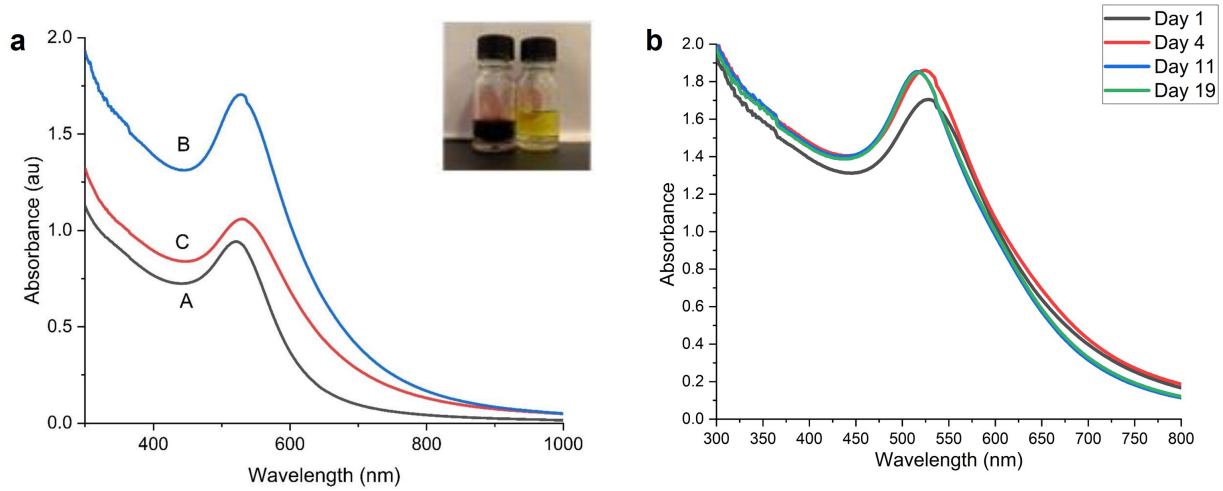

Figure 2. UV-Vis absorption spectra (a) of gold nanoparticles in the following GA/gold ratio: (A) 0.5 mL/1 mL, (B) 1.5 mL/1 mL, (C) 2 mL/1 mL; (b) of sample B at various times (days 1, 4, 11, and 19); insert: photos of gold salt (yellow colour), gold nanoparticles (dark purple)

Figure 2a shows the absorption spectra of the three samples, A, B, and C. The absorption spectra show a single SPR peak centered around 523 nm to 532 nm. A single SPR peak indicates that the NPs are close to spherical shape [16]. The SPR peak is red-shifted as the volume of the $HAuCl_4$ solution is increased from 0.5 mL to 2 mL to the fixed volume of 1 mL GA extract, indicating the formation of larger-size NPs. This size increase may be due to insufficient screening of the AuNPs by GA as the $HAuCl_4$ concentration increased [17]. By increasing the volume of $HAuCl_4$ from 0.5 mL (sample A) to 1.5 mL (sample B) to a fixed volume of 1 mL of GA extract, the absorption SPR peak increased, indicating the increasing concentration of AuNP [18]. These measurements were repeated for all the samples and showed consistent results, and no significant differences were observed.

The UV-Vis spectrum of sample B was examined on days 1, 4, 11, and 19 to determine the AuNPs stability. As shown in Figure 2b, a slight increase in the SPR band was noticed on day 4 relative to day 1. However, the absorption level was constant throughout days 11 and 19, indicating the completion of the reaction and the stability of the AuNPs. It was observed that the NPs were found to be stable for more than one month, with no noticeable variation in the SPR band, indicating no evidence for aggregation. GA is a weak cationic polyelectrolyte with positive ionic groups along the backbone or side chains. When adsorbed on a negative surface, it leads to steric stabilization. The hydroxyl groups in the GA network also hold the NPs through physical interactions. This allows the stabilization of NPs against aggregation [19]. Using pulsed laser ablation, Mzwd et al. [17] successfully synthesized AuNP with and without GA. The chemical constituents of GA significantly influenced the size and morphology of NPs [14].

The structure and size of the AuNPS were analyzed using TEM. The TEM images and corresponding particle size distribution for all samples are shown in Figure 3. TEM images and size distribution for the samples revealed spherical-shaped NPs. The average size of the particles is almost the same, and it was estimated to be around 15, where about 60% of the particles have shown size between 8–12 nm.

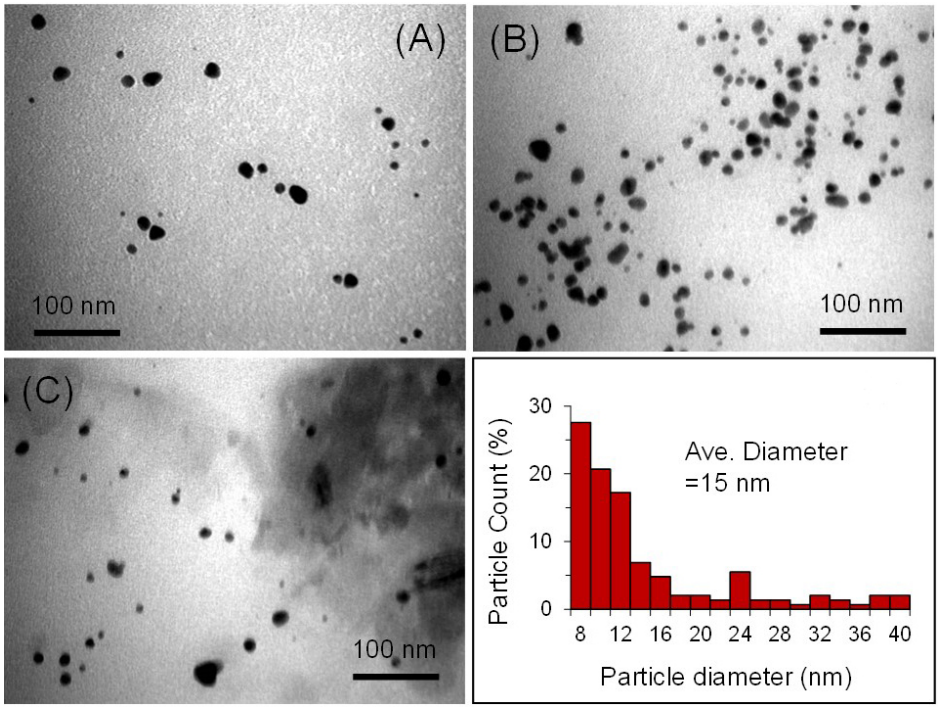

Figure 3. TEM images of GA-AuNPs for samples A, B, and C, and the particle size distribution (sample B, the image in the bottom right corner)

FTIR measurements were performed to identify possible interactions between AuNPs and GA molecules that are believed to be responsible for the reduction and capping. GA is a mixture of macromolecules of different sizes and compositions (mainly carbohydrates and proteins/polysaccharides). The spectra of GA and GA AuNPs are shown in Figure 4. The spectra of GA and GA-AuNPs show several functional groups such as carboxyl and hydroxyl that are responsible for the reduction of the gold salt and capping of the resulting NPs.

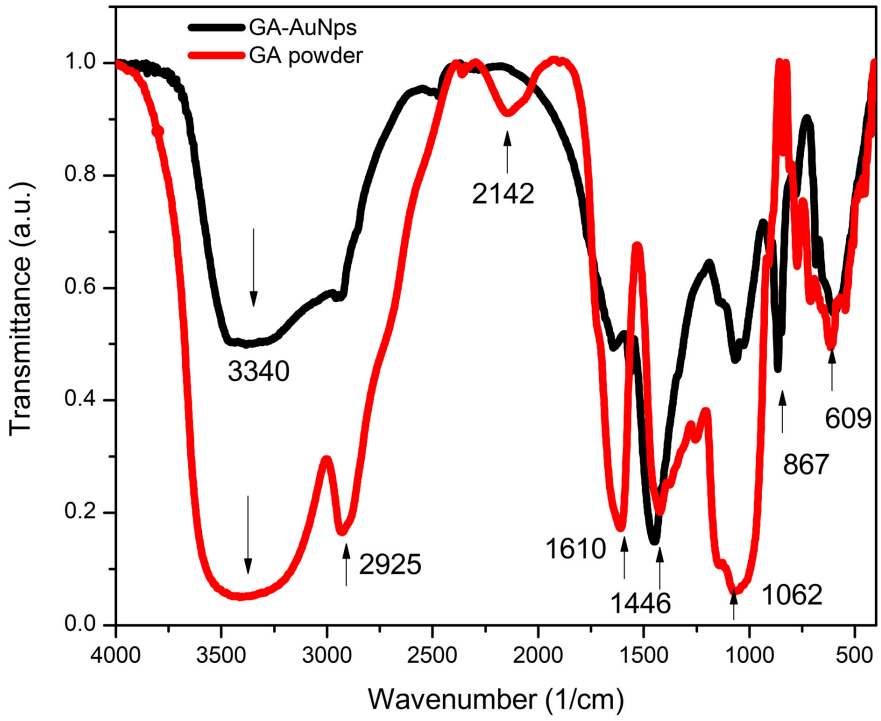

Figure 4. Normalized FTIR spectra of gum Arabic (black) and GA-AuNPs (red)

The broad peak at around 3,340 cm^{-1} is assigned to the N-H stretching vibration and the free O-H group. The peak at 2,925 cm^{-1} is associated with C-H stretching, and the band around 1,610 cm^{-1} corresponds to COO-symmetric stretching. The peak at 1,610 cm^{-1} is related to the C-O-C and C-OH vibrations of the protein/polysaccharide in GA. The peak at 1,446 cm^{-1} is assigned to COO- asymmetric stretching. The 1,200–900 cm^{-1} peaks are due to carbohydrates (polysaccharide structure). The peak at 867 cm^{-1} is attributed to the stretching vibration of the C-O bonds in the GA-AuNPs.

This peak is also present in pure GA but is more pronounced in GA-AuNPs due to capping of the NPs. The presence of this peak confirms the formation of GA-AuNPs composite. Overall, the slight shifts between the peak value of spectra for GA and GA-AuNPs suggest that the functional groups of GA are coordinated to the charged surface of the NP.

Fluorescence quenching

The fluorescence quenching properties of NPs can broaden the scope of their applications in various fields of medical science. One of the essential applications of fluorescence quenching is the ability to detect and sense chemical and biological molecules in solution [20]. Fluorescence quenching involves several processes that can lead to decreasing the fluorescence of a fluoroscope. The quenching occurs in various processes and involves numerous molecular interactions such as ground-state complex formation, collisional process, excited-stare reaction and Föster resonance energy transfer (FRET) [21]. FRET transfers energy from a donor with an excited molecule to a surrounding acceptor. This process is established non-radiatively through long-range dipole-dipole interactions [22]. This transfer can only occur when the acceptor's emission band overlaps with the absorption band of the donor molecule. The energy transfer rate depends on the sufficient overlap of the emission of the donor, the absorption of the acceptor, and the distance R_o between the donor and acceptor (typically in the range of 1–10 nm), the value of R_o and falling off at the rate of $1/R_O^6$. The transfer energy on the distance R_o is most efficient when the donor-acceptor distance is close [22].

Figure 5 illustrates the absorption spectrum of the acceptor, AuNPs (black line in arbitrary unit) and the emission fluorescence of the doner C153 dye (red line, arbitrary unit). As observed, the overlap region between both spectra is over a wide range from 514 nm to 593 nm. The overlapping is a requirement for an efficient energy transfer [23]. Using the spreadsheet made available by Visser et al. [24], the critical energy transfer distance R_o was calculated from the normalized fluorescence and absorption spectra and was determined to be 31.1 Å for the AuNP-C153 dye. Such a small value indicates efficient energy transfer between donor and acceptor molecules. The overlapping and small value of R_o requirement meets and leads to the conclusion that the excited state energy is expected to be transferred from the donner (dye) to the acceptor (AuNP) through non-radiative processes, FRET.

On the other hand, the decrease in fluorescence intensity of C153 may be attributed to excitation energy transfer between the dye and NPs through the formation of a complex ground state. In this respect, a transfer of energy from the single excited state of C153 to AuNPs is likely because the singlet excited state energy of C153 (3 eV) is significantly higher than the band gap energy of AuNPs (2.4 eV). If the AuNPs absorbed the fluorescence emission of the dye, a new emission band attributed to AuNPs would have been detected. Therefore, it can be seen from Figure 6 that such an emission peak is not observed. Hence, we conclude that the complex ground state, in this case, is not formed [25].

The quenching ability of the AuNPs was investigated by adding different volumes of AuNPs to a fixed volume of C153 dye, keeping the final volume constant. Figure 6 shows the fluorescence of the C153 dye at different volumes of AuNPs. It can be observed clearly that the fluorescence intensity of the dye decreased with increasing volumes of AuNPs, indicating a quenching process. It is worth mentioning that different volumes of distilled water up 10 mL were added to the dye without the presence of AuNPs, and no significant change in the fluorescence intensity was observed; we conclude that the observed quenching is due to the presence of AuNPs. The measurements were repeated for all concentrations, showing consistent results and no significant differences were observed. As explained above, we assume an energy transfer

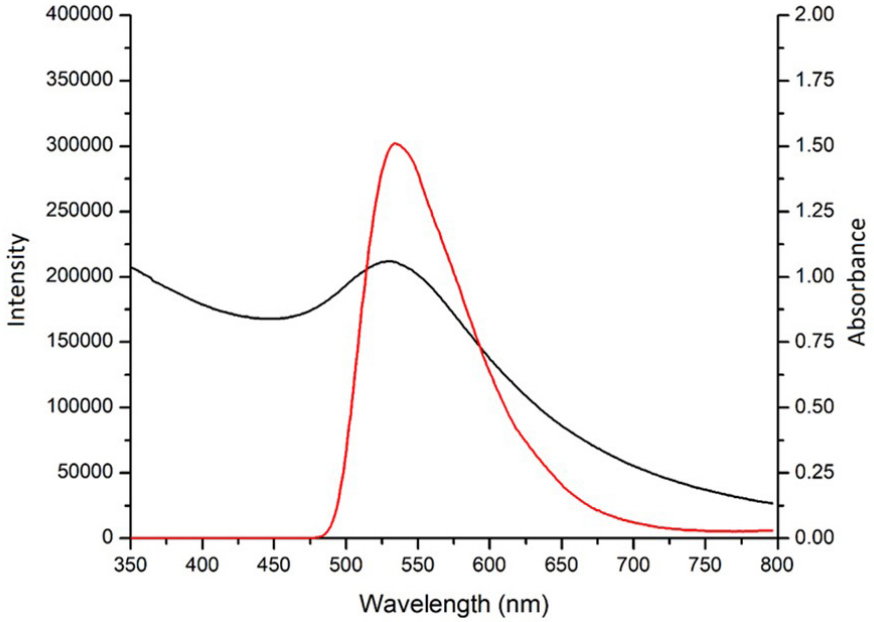

Figure 5. Overlapping of the absorption spectrum of the AuNPs (in black) with the emission spectrum of coumarin 153 dye (in red)

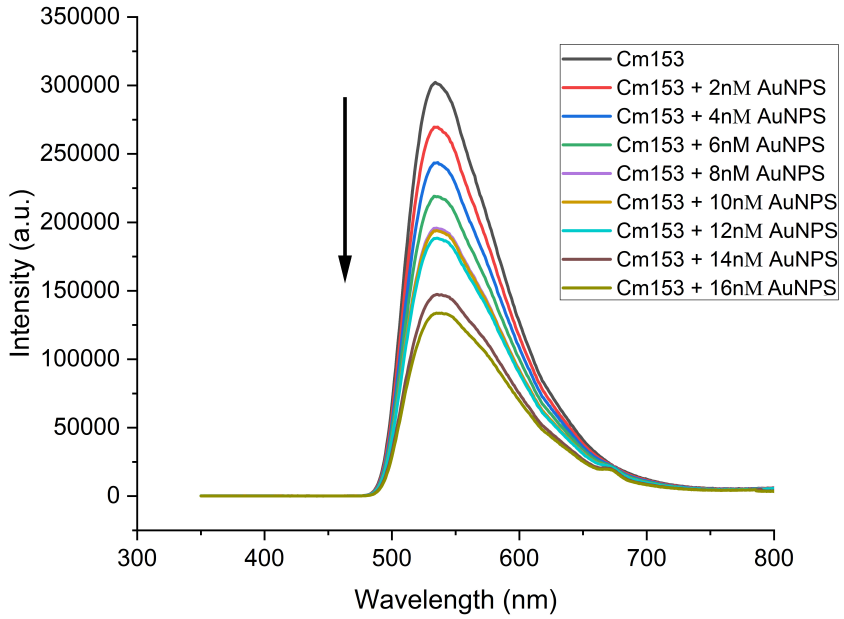

Figure 6. Fluorescence spectra of C153 dye with increasing amount of gold nanoparticles. Each spectrum is an average of three trials

occurred from the C153 to the AuNPs, likely via a dynamic mechanism. Static quenching was ruled out because no change in the fluorescence emission spectrum was observed, and no new absorption band was observed as an indication of ground state formation. Multiple reports proposed and confirmed the fluorescence quenching by binding probe molecules to the metal surface of the NPs [26, 27].

For dynamic quenching, the decrease in fluorescence intensity is described by the Stern-Volmer equation as,

$I_o/I = 1 + Ksv\,[Q]$ (1)

where I_o is the fluorescence of the dye without a quencher; I is the fluorescence of the dye with a quencher; [Q] is the concentration of the quencher (AuNPs), and Ksv is the Stern-Volmer quenching constant (quencher rate coefficient).

The Stern-Volmer plot of the quenching process of C153 is shown in Figure 7. The linearity of the plot indicates that only one type of quenching occurs in the system and suggests that dynamic quenching is the primary process. The Stern-Volmer equation plot was used to calculate the Stern-Volmer quenching constant and was found to be 1×10^6 M^{-1}. Such a high value suggests the adsorption of a large number of dye molecules to the surface of AuNPs via the O-atom of carbonyl [28].

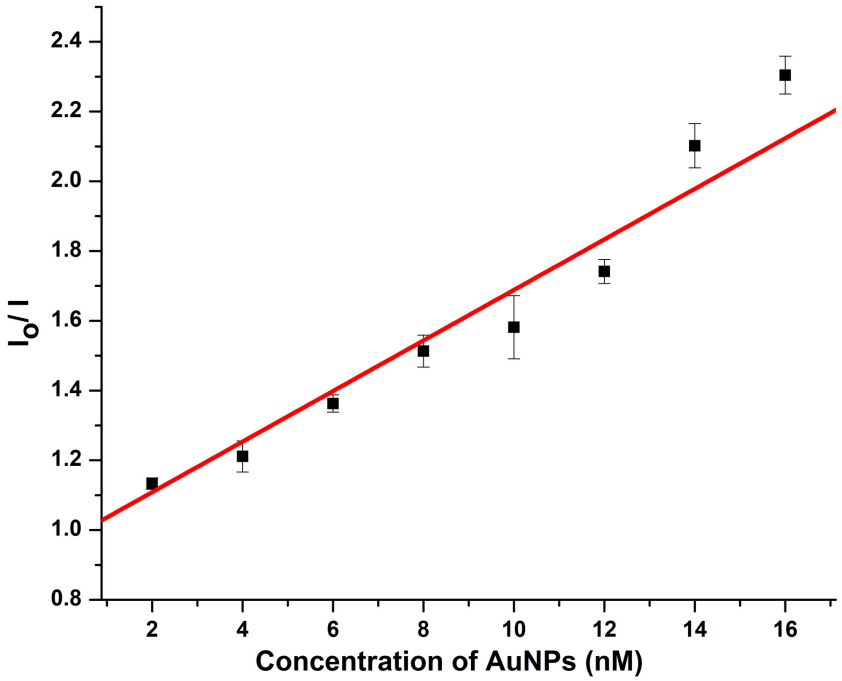

Figure 7. Stern-Volmer plots for fluorescence quenching of C153 dye at different concentrations of AuNPs

The fluorescence quenching recovery was investigated by adding different BSA volumes to the AuNP-C153 mixture. Figure 8 illustrates an increase in fluorescence intensity (recovery) upon adding different volumes of BSA to the dye-NP system. A slight shift of the peak observed may be attributed to aggregation [18].

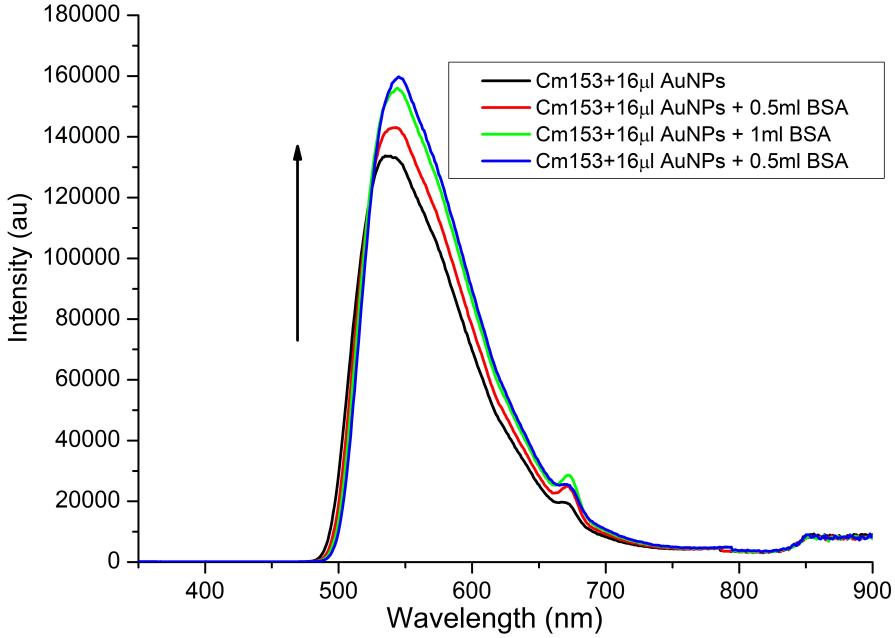

Figure 8. Effect of BSA on the recovery of fluorescence of C153-AuNP. Each spectrum is an average of three trials

A possible explanation for the BSA effect is its affinity with AuNPs to form complex-combined structures through adsorbing onto the surface of AuNPs that might have detached the C153 molecules from the AuNPs' surface results on the free C153 molecules, which are highly fluorescent [12]. The AuNP-BSA structures may also aggregate, increasing the distance from the C153 molecules, subsequently leading to the C153 fluorescence recovery [23]. This fluorescence recovery process may be used to detect and identify proteins in the buffer and serum. However, further experimentation is required to assess the variations of fluorescence recovery for various proteins. The process of fluorescence quenching using the dye and recovery by the protein is illustrated in Figure 9.

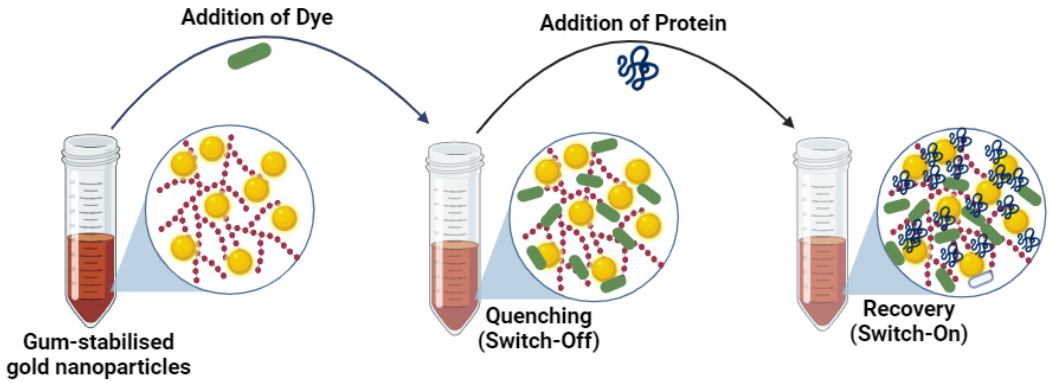

Figure 9. Illustration of fluorescence quenching and recovery by the GA-AuNPs system

Discussion

This study reports the synthesis of AuNPs using a green method utilizing GA extract as a reducing and stabilizing agent. The formation of GA-AuNPs was confirmed by visual observation, UV-Vis spectroscopy, TEM, and FTIR. The SPR was around 523 nm to 532 nm. UV-Vis spectroscopy and TEM results show the spherical shape of NPs with an average size of 15 nm. FTIR revealed the functional groups of GA are coordinated to the charged surface of the NP. The effect of GA-AuNPs on the fluorescence of C153 was investigated and revealed that the fluorescence from C153 was effectively quenched. The quenching of C153 followed the Stern-Volmer quenching model. The energy transfer between C153 and GA-AuNPs is correlated to a dynamic mechanism (FRET). The fluorescence of AuNP-C153 mixture was recovered upon adding BSA. This fluorescence turn-off/on will facilitate the development of a detection system for detecting and identifying different proteins in the buffer and serum. These experiments are crucial to precisely calculate the fluorescence recovery levels for discrimination of proteins and buffers.

Overall, the paper's novelty lies in combining the green synthesis of AuNPs using GA extract and the demonstration of fluorescence quenching of C153 dye and its recovery properties for protein detection. This study contributes to developing sustainable and efficient NP synthesis methods and offers potential applications in biosensing and optoelectronic devices.

Abbreviations

AuNPs: gold nanoparticles

BSA: bovine serum albumin

C153: coumarin 153

FRET: Föster resonance energy transfer

FTIR: Fourier transform infrared

GA: gum Arabic

$HAuCl_4$: gold (III) chloride trihydrate

NPs: nanoparticles

SPR: surface plasmon resonance

TEM: transmission electron microscopy

UV-Vis: ultra-violet-visible

Declarations

Acknowledgments

Ms. Fatima AlHannan, the laboratory manager is thanked for her help in the procurement of materials.

Author contributions

ATA and OSE equally contributed to: Investigation, Writing—original draft. DAK: Investigation. GRD: Data curation, Writing—review & editing. SA: Conceptualization, Data curation. FZH: Conceptualization, Validation, Writing—review & editing, Supervision. All authors read and approved the submitted version.

Conflicts of interest

The authors declare that they have no conflicts of interest.

Ethical approval

Not applicable.

Consent to participate

Not applicable.

Consent to publication

Not applicable.

Availability of data and materials

The raw data of absorption and fluorescence spectroscopy and Origin files are available with the corresponding author.

Funding

Financial support through Research Summer School [2223] is gratefully acknowledged. The funders had no role in study design, data collection and analysis, decision to publish, or preparation of the manuscript.

References

1. Khan F, Shariq M, Asif M, Siddiqui MA, Malan P, Ahmad F. Green Nanotechnology: Plant-Mediated Nanoparticle Synthesis and Application. Nanomaterials (Basel). 2022;12:673. [DOI] [PubMed] [PMC]
2. Duan H, Wang D, Li Y. Green chemistry for nanoparticle synthesis. Chem Soc Rev. 2015;44:5778–92. [DOI] [PubMed]
3. Jadoun S, Arif R, Jangid NK, Meena RK. Green synthesis of nanoparticles using plant extracts: a review. Environ Chem Lett. 2021;19:355–74. [DOI]
4. Sathishkumar M, Sneha K, Won SW, Cho CW, Kim S, Yun YS. Cinnamon zeylanicum bark extract and powder mediated green synthesis of nano-crystalline silver particles and its bactericidal activity. Colloids Surf B Biointerfaces. 2009;73:332–8. [DOI] [PubMed]
5. Philip D. Green synthesis of gold and silver nanoparticles using *Hibiscus rosa sinensis*. Physica E Low Dimens Syst Nanostruct. 2010;42:1417–24. [DOI]

6. Shankar SS, Ahmad A, Sastry M. Geranium leaf assisted biosynthesis of silver nanoparticles. Biotechnol Prog. 2003;19:1627–31. [DOI] [PubMed]
7. Eskandari-Nojehdehi M, Jafarizadeh-Malmiri H, Jafarizad A. Microwave Accelerated Green Synthesis of Gold Nanoparticles Using Gum Arabic and their Physico-Chemical Properties Assessments. Zeitschrift für Physikalische Chemie. 2018;232:325–43. [DOI]
8. Joshita D, Cholimi S, Purnamasari P, Pujiyanto A. Antioxidant activity of gold nanoparticles using gum arabic as a stabilizing agent. Int J Pharm Pharm Sci. 2014;6:462–5.
9. Huang X, El-Sayed MA. Gold nanoparticles: Optical properties and implementations in cancer diagnosis and photothermal therapy. J Adv Res. 2010;1:13–28. [DOI]
10. Tiwari PM, Bawage SS, Singh SR. 13 - Gold nanoparticles and their applications in photomedicine, diagnosis and therapy. In: Hamblin MR, Avci P, editors. Applications of Nanoscience in Photomedicine. Oxford: Chandos Publishing; 2015. pp. 249–66. [DOI]
11. Swierczewska M, Lee S, Chen X. The design and application of fluorophore-gold nanoparticle activatable probes. Phys Chem Chem Phys. 2011;13:9929–41. [DOI] [PubMed] [PMC]
12. De M, Rana S, Akpinar H, Miranda OR, Arvizo RR, Bunz UH, et al. Sensing of proteins in human serum using conjugates of nanoparticles and green fluorescent protein. Nat Chem. 2009;1:461–5. [DOI] [PubMed] [PMC]
13. Gavrilaş S, Ursachi CŞ, Perţa-Crişan S, Munteanu FD. Recent Trends in Biosensors for Environmental Quality Monitoring. Sensors (Basel). 2022;22:1513. [DOI] [PubMed] [PMC]
14. Saha K, Agasti SS, Kim C, Li X, Rotello VM. Gold nanoparticles in chemical and biological sensing. Chem Rev. 2012;112:2739–79. [DOI] [PubMed] [PMC]
15. ElMitwalli OS, Barakat OA, Daoud RM, Akhtar S, Henari FZ. Green synthesis of gold nanoparticles using cinnamon bark extract, characterization, and fluorescence activity in Au/eosin Y assemblies. J Nanopart Res. 2020;22:309. [DOI]
16. Srinath BS, Ravishankar Rai V. Biosynthesis of highly monodispersed, spherical gold nanoparticles of size 4-10 nm from spent cultures of Klebsiella pneumoniae. 3 Biotech. 2015;5:671–6. [DOI] [PubMed] [PMC]
17. Mzwd E, Ahmed NM, Suradi N, Alsaee SK, Altowyan AS, Almessiere MA, et al. Green synthesis of gold nanoparticles in Gum Arabic using pulsed laser ablation for CT imaging. Sci Rep. 2022;12:10549. [DOI] [PubMed] [PMC]
18. Memon AG, Channa IA, Shaikh AA, Ahmad J, Soomro AF, Giwa AS, et al. Citrate-Capped AuNP Fabrication, Characterization and Comparison with Commercially Produced Nanoparticles. Crystals. 2022;12:1747. [DOI]
19. Putro JN, Lunardi VB, Soetaredjo FE, Yuliana M, Santoso SP, Wenten IG, et al. A Review of Gum Hydrocolloid Polyelectrolyte Complexes (PEC) for Biomedical Applications: Their Properties and Drug Delivery Studies. Processes. 2021;9:1796. [DOI]
20. Chen L, McBranch DW, Wang HL, Helgeson R, Wudl F, Whitten DG. Highly sensitive biological and chemical sensors based on reversible fluorescence quenching in a conjugated polymer. Proc Natl Acad Sci U S A. 1999;96:12287–92. [DOI] [PubMed] [PMC]
21. Amjadi M, Farzampour L. Fluorescence quenching of fluoroquinolones by gold nanoparticles with different sizes and its analytical application. J Lumin. 2014;145:263–8. [DOI]
22. Swider E, Maharjan S, Houkes K, van Riessen NK, Figdor C, Srinivas M, et al. Förster Resonance Energy Transfer-Based Stability Assessment of PLGA Nanoparticles in Vitro and in Vivo. ACS Appl Bio Mater. 2019;2:1131–40. [DOI] [PubMed] [PMC]
23. Cardullo RA. Theoretical principles and practical considerations for fluorescence resonance energy transfer microscopy. Methods Cell Biol. 2007;81:479–94. [DOI] [PubMed]
24. Visser AJWG, Vysotski ES, Lee J. Critical Transfer Distance Determination Between FRET Pairs [Internet]. c2011 [cited 2022 Sep 14]. Available from: http://photobiology.info/Experiments/Biolum-Expt.html

25. Desai VR, Hunagund SM, Pujar MS, Basanagouda M, Kadadevarmath JS, Sidarai AH. Spectroscopic interactions of titanium dioxide nanoparticles with pharmacologically active 3(*2H*)-pyridazinone derivative. J Mol Liq. 2017;233:166–72. [DOI]
26. Błaszkiewicz P, Kotkowiak M, Dudkowiak A. Fluorescence quenching and energy transfer in a system of hybrid laser dye and functionalized gold nanoparticles. J Lumin. 2017;183:303–10. [DOI]
27. Kang KA, Wang J, Jasinski JB, Achilefu S. Fluorescence manipulation by gold nanoparticles: from complete quenching to extensive enhancement. J Nanobiotechnology. 2011;9:16. [DOI] [PubMed] [PMC]
28. Ghosh SK, Pal A, Kundu S, Nath S, Pal T. Fluorescence quenching of 1-methylamino pyrene near gold nanoparticles: size regime dependence of the small metallic particles. Chem Phys Lett. 2004;395: 366–72. [DOI]